ISSN 0038-0946, Solar System Research, 2025, Vol. 59:26. © Pleiades Publishing, Ltd., 2025.

Method of Checking the Spectral Sensitivity of Optical Paths of the Sun-Terahertz Scientific Instrumentation in the Frequency Range 0.4–20 THz

M. V. Philippov[a, *, **], V. S. Makhmutov[a], M. V. Razumeyko[a], G. I. Kropotov[b], and V. A. Nikolaev[b]

[a] *Lebedev Physical Institute (LPI RAS), Russian Academy of Sciences (FIAN), Moscow, Russia*

[b] *Tydex, LLC, St. Petersburg, Russia*

**e-mail: mfilippov@frtk.ru*

***e-mail: filippovmv@lebedev.ru*

Received November 8, 2024; revised November 20, 2024; accepted December 3, 2024

Abstract—The paper describes the Sun-Terahertz space experiment, planned for 2025–2027 on board the Russian segment of the International Space Station. The goals of the experiment are to obtain data on the Sun's terahertz radiation, as well as to study solar active regions and solar flares. The scientific equipment of the Sun-Terahertz consists of eight detection channels, which are sensitive to radiation of different frequencies in the range of 0.4–12.0 THz. The purpose of this work is to check the compliance of the actual spectral characteristics of scientific equipment with the calculated ones in the operating frequency range of 0.4–20 THz using auxiliary equipment and the developed methodology.

Keywords: Sun, solar flares, terahertz radiation, optical system, Golay cell

DOI: 10.1134/S0038094624601683

INTRODUCTION

The Sun is a source of electromagnetic radiation in a wide range of frequencies and energies. Currently, ground-based and exoatmospheric observations of radiation are carried out in almost the entire solar spectrum (Kinnison et al., 2020; Howard et al., 2013; Domingo et al., 1995; Davila et al., 1996) with the exception of radiation in the terahertz range, since it is almost completely absorbed by the Earth's atmosphere, except for a transparency window with a central frequency of about 30 THz (Kaufmann et al., 2015). The Sun-Terahertz space experiment is aimed at studying solar flare radiation in the terahertz range (Kalinin et al., 2021). The main goal of the experiment is to obtain new experimental data for the development and further development of models of the physical mechanism of the occurrence of powerful solar proton flares and their prediction (Kaufmann et al., 1985, 2001, 2003, 2004; Kaufmann, 1996; Krucker et al., 2013; Luthi et al., 2004; Makhmutov et al., 2003; Makhmutov et al., 2011). The Sun-Terahertz space experiment will study the Sun's terahertz radiation in order to determine the physical nature of solar flares and develop a method for predicting them.

The study of solar flares at different frequencies allows us to investigate processes occurring at different levels of the solar atmosphere. For example, data on submillimeter solar radiation make it possible to study the processes of acceleration and transfer of energetic electron flows in the lower layers of the solar atmosphere from the transition region to the chromosphere (Wedemeyer et al., 2016). Some flares have a second spectral component: instead of the expected decrease in gyrosynchrotron radiation fluxes with increasing frequency, their growth is observed at frequencies of 212, 405 GHz and higher (Kaufmann et al., 2004; Krucker et al., 2013). Obtaining new experimental data, especially in the terahertz range of waves of the order of 1–10 THz, will make it possible to study the characteristics and physical nature of this feature of the frequency spectrum and determine the frequency at which changes in the slope of the spectrum occur in various solar flares.

EQUIPMENT FOR THE SUN-TERAHERTZ EXPERIMENT

The Sun-Terahertz scientific apparatus (Fig. 1) consists of eight detection channels (detectors) sensitive to radiation in the vicinity of frequencies of 0.4, 0.7, 1.0, 3.0, 5.0, 7.0, 10.0, and 12.0 THz.

Each radiation detector consists of the following components:

— An optical telescope (Kvashnin et al., 2021) that concentrates radiation into a receiver.

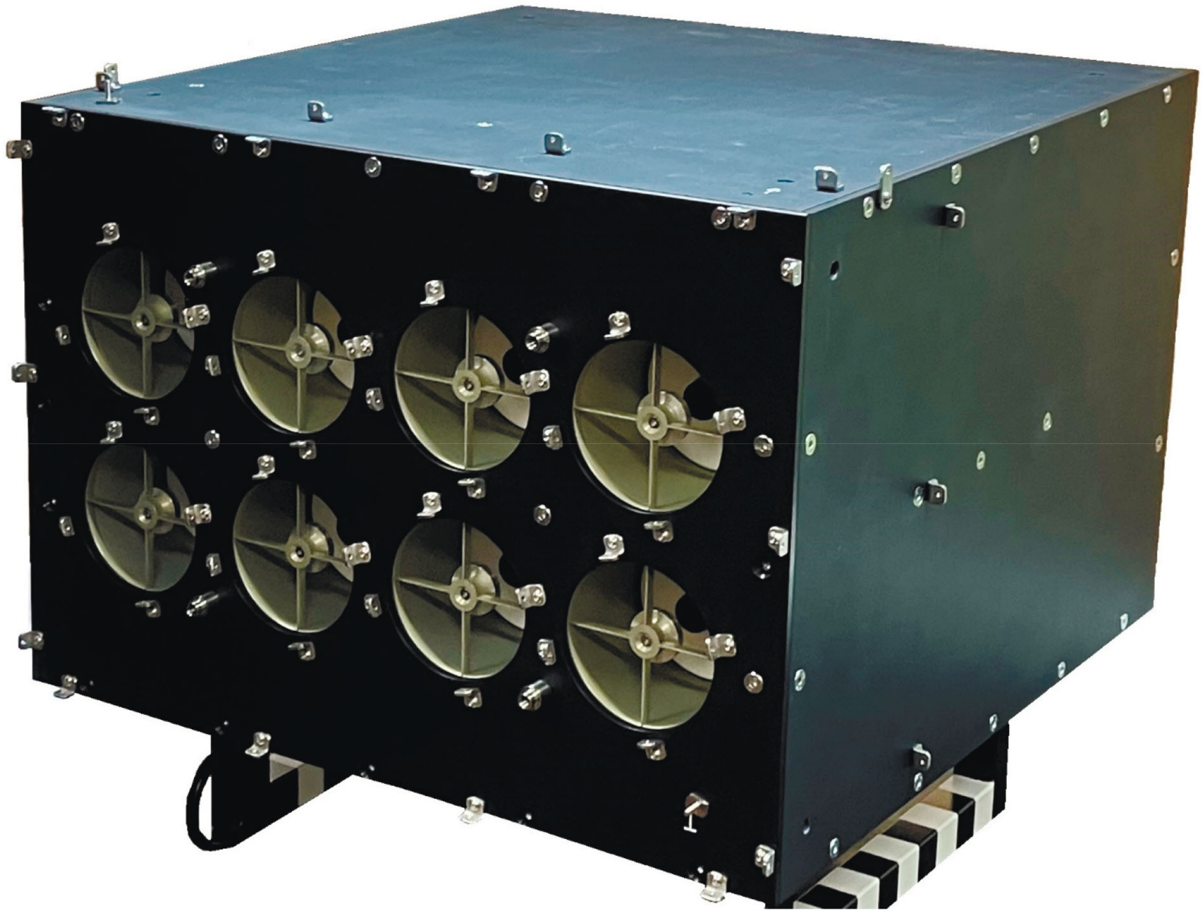

Fig. 1. Photograph of the Sun-Terahertz scientific apparatus: view from the front panel. Shown are the telescope entrance windows, small and large mirrors.

— A system of successive filters that passes radiation in a given frequency range for each receiver, which consists of a low-pass filter LPF 23.1 (https://www.tydexoptics.com/pdf/ru/THz_Low_-Pass_Filter.pdf) and a band-pass filter BPF (http://www.tydexoptics.com/ru/products/tgc-ustrojstva/thz_band_pass_filter/) and thus ensures selectivity;

— An optical chopper that modulates the radiation in the input window of the receiver with a frequency of 10 Hz (Philippov et al., 2023a).

— A receiver, in the body of which an optoacoustic converter (OAC) “Golay cell” and an amplifier are placed (Kaufmann et al., 2014; Kropotov and Kaufmann, 2013; Philippov et al., 2023b, 2024a, 2024b).

The scientific equipment electronics unit is a set of electronic boards that provide: power supply, amplification of OAC signals, digitization, primary processing and transmission of data to the ISS, etc. (Philippov et al., 2023b).

The onboard implementation of the Sun-Terahertz space experiment is planned for 2025–2027.

The auxiliary equipment used in the experiment includes a single-channel detector model and a blackbody simulator (BBS) (Philippov et al., 2023b).

SENSITIVITY OF RECEIVERS OF THE FLIGHT MODEL OF SCIENTIFIC EQUIPMENT

Using a single-channel layout for the receiver a series was conducted measurements of the peak-to-peak noise signal (with an aluminum plug installed in the input window of the receiver under test) at different room temperatures. The data are presented in Table 1. In the first column is the measurement number, in the second column the average temperature on the OAC case, in the third column the average amplitude of the receiver noise signal. The last line (1–7) shows the results obtained from a set of seven measurements.

As can be seen, the correlation between the temperature on the OAC case and the noise signal amplitude (with temperature changes in the range of 4°C) is absent, therefore, further the receiver's own noise, caused primarily by the amplifier, will be considered constant within the operating temperatures of the OAC, and the measured average value of the receiver's own noise: U_G (noise) = (38.42 ± 21.77) mV.

Thus, it is possible to estimate the minimum signal to which the equipment receivers are sensitive as the value U_G (noise).

CHECKING THE SPECTRAL CHARACTERISTICS OF THE DETECTOR USING A SINGLE-CHANNEL LAYOUT AND BBS IN THE RANGE OF 0.4–20 THz

In this experiment, the dependence of the receiver output signal at a fixed temperature of the BBS emitter was investigated: T_{bb} = 873 K for cases of single and double installed LPF 23.1 filters.

The essence of the method is to measure the ratio of the receiver signal swing for a single LPF 23.1 cutoff filter at the maximum high temperature that the BBS can support for a long time (U_G (873 K)) and the receiver signal swing for a dual (two consecutive sets) LPF 23.1 cutoff filter (U_G^1 (873 K)).

Since the receiver signal is proportional to the magnitude of the input radiation flux, it can be assumed that the ratio of the receiver signal amplitude will be equal to the ratio of the calculated radiation fluxes for a single (Φ_R (873 K)) and a double cut-off filter LPF 23.1 (Φ_R^1 (873 K)).

The optical paths of the detectors include: a telescope with two mirrors, a cutting filter LPF 23.1, a bandpass filter BPF, and the spectral characteristics of the input window OAC also have an effect. The resulting spectral characteristic of the optical path is obtained by multiplying the spectral characteristics of transmission and reflection (for mirrors). Spectral characteristics as a dependence of the transmittance or reflection coefficient on the radiation wavelength were obtained at Tydex, LLC. Transmission spectra LPF 23.1 cut-off filter and bandpass filters BPF 1.0–BPF 12.0 were measured using a Bruker VERTEX 70 spectrometer, and the spectra of bandpass filters BPF 0.4 and BPF 0.7 were measured using a Menlo Systems TERA K8 spectrometer (Kropotov et al., 2023). To reduce the influence of instrumental noise, measurements are taken four times and then averaged at each point. Thus, the initial spectral characteristic is obtained. Next, the original characteristic files from the wavelength grid are converted to a frequency grid with a step of 0.01 THz (intermediate values are obtained by linear interpolation) in the range from 0.01 to 2000 THz.

The level of instrumental noise of the measuring equipment is estimated as follows: the sections of the spectra in which the spectral transmittance (or reflection) coefficients of the studied samples tend to zero are considered. Among the values close to zero, there are also negative values, which are a consequence of instrumental noise or bias in the amplification stages of the measuring equipment. Characteristic value: 5×10^{-4} rel. units.

Table 1. Measured values of the noise signal peak-to-peak for the receiver No. GC00284 at different OAC case temperatures

Measurement number	T_G, °C	U_G (noise), mV
1	21.92 ± 0.27	38.75 ± 21.91
2	22.55 ± 0.27	38.69 ± 22.14
3	23.15 ± 0.25	38.50 ± 21.76
4	23.69 ± 0.22	38.77 ± 21.84
5	24.22 ± 0.24	38.82 ± 22.04
6	25.07 ± 0.30	38.15 ± 21.59
7	25.96 ± 0.21	37.99 ± 21.64
1–7	24.14 ± 1.23	38.42 ± 21.77

Since the spectral density of the radiation fluxes of the quiet atmosphere of the Sun increases with increasing frequency, the multiplication of small values of the spectral transmittance coefficient, which is instrumental noise, by large values of the radiation flux densities can make a significant contribution to the error in the calculated solar radiation fluxes. To reduce this effect, each spectral characteristic undergoes additional processing: the value 5×10^{-4} is subtracted from each point, after which all negative values are set to zero.

Returning to the method of measuring the ratio of signal peak-to-peak values for single and double LPF 23.1 filters in the optical path of the detector: to compensate for the temperature effect of the OAC, all measured values should be reduced to the same temperature on the OAC body according to formula (1) (Philippov et al., 2024b)

$$U_G\left(T_{bb}, T_{G2}\right) = \frac{U_G\left(T_{bb}, T_{G1}\right)}{1 - \gamma_G \Delta T_G}, \quad (1)$$

where $\left(T_{bb}, T_{G01}\right)$ is the measured receiver signal swing (mV) at the BBS emitter temperature: T_{bb} and temperature T_{G1} on the OAC body, mV; $U_G\left(T_{bb}, T_{G2}\right)$ is the temperature-corrected receiver signal swing (mV); $\Delta T_G = T_{G2} - T_{G1}$; T_{G2} = 25°C; γ_G = (–3.52 ± 0.06)% per 1°C.

However, as shown in Table 1, the receiver's own noise is almost independent of temperature. Thus, to increase the accuracy of the calculation, the signal amplitude should be conditionally divided into two components: the useful signal and the characteristic constant noise signal, and a temperature correction should be made only for the difference between the useful and noise signals. Formula (1), taking into account the noise component of the signal, takes the following form:

$$U_G(T_{bb}, T_{G2}) = \frac{U_G(T_{bb}, T_{G1}) - \gamma_G \Delta T_G U_G(\text{noise})}{1 - \gamma_G \Delta T_G}, \quad (2)$$

where $U_G(\text{noise}) = (38.42 \pm 21.77)$ mV.

Standard deviation $\sigma U_G(T_{bb}, T_{G2})$ receiver signal amplitude at temperature $T_{G2} = 25°C$ on the OAC body is converted from the standard deviation $\sigma U_G(T_{bb}, T_{G1})$ signal amplitude at temperature T_{G1} on the OAC body similarly:

$$\sigma U_G(T_{bb}, T_{G2}) = \frac{\sigma U_G(T_{bb}, T_{G1}) - \gamma_G \Delta T_G \sigma U_G(\text{noise})}{1 - \gamma_G \Delta T_G}. \quad (3)$$

It should also be noted that in addition to the fact that the BBS emitter is not a black body (the blackness degree in the terahertz wavelength range is not less than 0.88), it is necessary to take into account the air gap (approximately 0.6 m) between the BBS emitting element and the input window of the receiver, since terahertz radiation in the range of 1–10 THz experiences significant attenuation (from 100 dB/km to more than 100000 dB/km depending on the frequency) due to absorption by air molecules (Cui et al., 2011; Yasuko and Takamasa, 2008).

The radiation flux from the BBS passing through the receiver input window F_R (W), is equal to

$$\Phi_R(T_{bb}) = S_{tel} \int_{\nu_1}^{\nu_2} d(\nu)\, r(\nu, T_{bb})\, t(\nu)\, a(\nu)\, d\nu, \quad (4)$$

where S_{tel} is the area of the telescope entrance window ($S_{tel} = 3.84 \times 10^{-3}$ m^2); ν is the radiation frequency (Hz) ($\nu_1 = 0.01$ THz, $\nu_2 = 2000$ THz); $d(\nu)$ is the spectral coefficient of diffraction losses on the telescope mirrors; $r(\nu, T_{bb})$ is the spectral density of radiation per unit area in the frequency range (ν; dν), W/(m^2 Hz); $t(\nu)$ is the transmittance of the detector optical path: telescope, filter system and OAC input window; $a(\nu)$ is the spectral coefficient that determines absorption of radiation in air.

Figure 2 shows the transmission spectra of the optical paths of the detectors at 0.4, 5.0, and 10.0 THz using a single cutoff filter LPF 23.1 (blue curve) and a double filter LPF 23.1 (red curve), taking into account the absorption of radiation in air.

Preliminary conclusions can be made that for channels at 0.4, 0.7 and 1.0 THz, when using a double filter LPF 23.1, the transmittance is reduced by about 70%, but the selectivity of the channels by radiation frequency increases sharply. Therefore, for these channels it is possible to use the double filter LPF 23.1 as a standard in the scientific instrumentation. For channels at 3.0, 5.0, 7.0 THz, using a double LPF 23.1 filter would not be advisable, but possible. For channels at 10.0 and 12.0 THz, due to the extremely low transmittance and its shift to the nontarget frequency range, the use of a double LPF 23.1 filter is impossible.

Table 2 shows the results of measurements of the signal amplitude of the receiver with single and double cutoff filters. The first column shows the channel numbers. The second column contains the measured value of the receiver signal amplitude (U_G, mV) at a BBS emitter temperature of T_{bb} = 873 K, a single bandpass filter and temperature on the OAC case of 25°C. The third column contains the measured value of the receiver signal amplitude (U_G^1, mV) at the BBS emitter temperature of T_{bb} = 873 K, a dual bandpass filter and a temperature of 25°C on the OAC case. The average values obtained during the experiment normalized to a temperature of 25°C according to formula (2) were taken as the measured values of the signal amplitude. The fourth column shows the signal swing ratio with a single LPF 23.1 cutoff filter installed to the signal amplitude with the dual LPF 23.1 filter installed. The fifth column shows the ratio of the radiation flux from the BBS calculated using formula (4) with a single LPF 23.1 cutoff filter installed to the radiation flux with a double LPF 23.1 filter installed, calculated in the range 0.01–2000 THz. The sixth column shows the ratio of the calculated values of radiation fluxes from the BBS at a temperature of T_{bb} = 873 K and a single LPF 23.1 filter installed. $\Phi_R^2(873\text{ K})$ is the radiation flow from the BBS entering the OAC, calculated in the frequency range 0.01–20 THz. $\Phi_R(873\text{ K})$ is the radiation flow from the BBS entering the OAC and calculated in the frequency range of 0.01–2000 THz.

The value of $\Phi_R^2(873\text{ K})/\Phi_R(873\text{ K})$ is close to unity (0.98–0.99), thus, according to the calculation, for each channel the scientific equipment is sensitive only to radiation lying in the approximate range of 0.01–20 THz. The remaining radiation from the BBS is almost completely scattered by the elements of the optical paths.

The ratio of the signal amplitudes agrees with sufficient accuracy (within the standard deviations) with the ratio of the incoming radiation fluxes. In this regard, it can be concluded that the actual spectral throughput characteristics of optical paths do not contradict the original measured and calculated parameters.

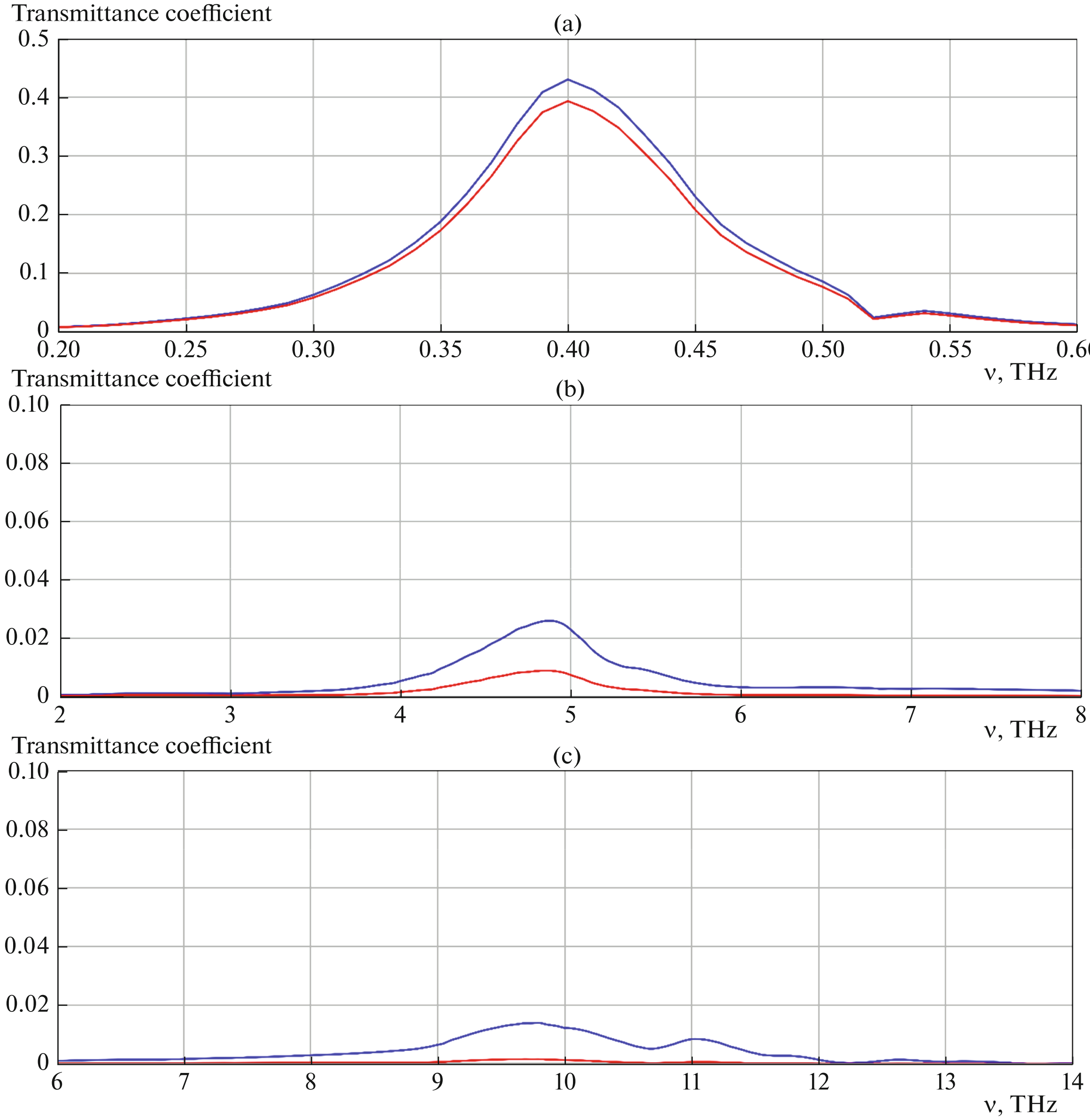

Fig. 2. Transmission spectrum of optical paths of detectors with a single LPF 23.1 filter (blue curve) and a double LPF 23.1 filter (red curve) installed, taking into account absorption in air: (a) at 0.4 THz; (b) at 5.0 THz; (c) at 10.0 THz.

Table 2. Results of measurements of the receiver signal swing with single and double cutoff filters

Channel number	U_G (873 TO), mV	U_G^1 (873 K), mV	U_G/U_G^1	Φ_R (873 K)/ Φ_R^1 (873 K)	Φ_R^2 (873 K)/ Φ_R (873 K)
1	5296.68 ± 90.40	493.25 ± 90.87	10.74 ± 2.17	11.44 ± 1.04	0.98 ± 0.09
2	3284.88 ± 57.13	202.86 ± 87.55	16.19 ± 7.27	10.32 ± 0.92	0.98 ± 0.09
3	3919.08 ± 161.89	324.04 ± 101.11	12.09 ± 4.27	8.03 ± 0.71	0.98 ± 0.09
4	9139.36 ± 75.83	894.55 ± 81.84	10.22 ± 1.01	8.64 ± 0.76	0.98 ± 0.09
5	12016.99 ± 80.87	1572.68 ± 34.85	7.64 ± 0.20	7.52 ± 0.66	0.98 ± 0.09
6	12164.82 ± 51.14	1249.19 ± 35.17	9.74 ± 0.32	9.53 ± 0.84	0.98 ± 0.09
7	9232.31 ± 120.32	681.11 ± 26.37	13.55 ± 0.70	13.01 ± 1.19	0.99 ± 0.09
8	11014.04 ± 102.75	491.95 ± 106.63	22.39 ± 5.06	17.28 ± 1.70	0.98 ± 0.14

CONCLUSIONS

This paper provides a brief description of the scientific equipment for the Sun-Terahertz experiment planned on board the Russian segment of the ISS. The main objective of the experiment is to study the Sun in the terahertz radiation range.

A method for checking the compliance of the calculated characteristics of the optical paths of scientific equipment with experimental data was developed and tested. This technique is suitable for testing OAC Golay cell based receivers in any target frequency range.

As calculations show, scientific equipment is sensitive to radiation in the frequency range of 0.01–20 THz, which satisfies the conditions of the upcoming experiment. Taking into account the approximate (within the standard deviations) equality of the ratios $U_{\rm G}/U_{\rm G}^1$ and $\Phi_{\rm R}\,(873\ {\rm K})/\Phi_{\rm R}^1\,(873\ {\rm K})$ we can conclude that the ratio $\Phi_{\rm R}^2\,(873\ {\rm K})/\Phi_{\rm R}\,(873\ {\rm K})$ is also calculated correctly.

FUNDING

This work was financed from the organization's budget. No additional grants were received to support this research.

CONFLICT OF INTEREST

The authors of this work declare that they have no conflicts of interest.

REFERENCES

Cui, H., Yao, J., and Wan, Ch., The study on THz wave propagation feature in atmosphere, *J. Phys. Conf. Ser.,* 2011, vol. 276, p. 012225. https://doi.org/10.1088/1742-6596/276/1/012225

Davila, J.M., Rust, D.M., Pizzo, V.J., and Liewer, P.C., Solar Terrestrial Relations Observatory (STEREO), in *Proc. SPIE's 1996 Int. Symp. Optical Sci. Engineering and Instrumentation,* 1996, vol. 2804. https://doi.org/10.1117/12.259724

Domingo, V., Fleck, B., and Poland, A.I., SOHO: The Solar and Heliospheric Observatory, *Space Sci. Rev.,* 1995, vol. 72, pp. 81–84. https://doi.org/10.1007/BF00768758

Howard, R.A., Vourlidas, A., Korendyke, C.M., et al., The solar and heliospheric imager (SoloHI) instrument for the Solar Orbiter mission, *Sol. Phys. Space Weather Instrum.,* 2013, vol. 8862, p. 88620H. https://doi.org/10.1117/12.2027657

Kalinin, E.V., Philippov, M.V., Makhmutov, V.S., Maksumov, O.S., Stozhkov, Yu.I., Kvashnin, A.A., Izmailov, G.N., and Ozolin, V.V., A study of the characteristics of a terahertz radiation detector for the Solntse–Terahertz scientific apparatus, *Cosmic Res.,* 2021, vol. 59, no. 1, pp. 1–5. https://doi.org/10.1134/S0010952521010032

Kaufmann, P., Submillimeter/IR solar bursts from high energy electrons, *Proc. AIP Conf.,* 1996, vol. 374, pp. 379–392. https://doi.org/10.1063/1.50945

Kaufmann, P., Correia, E., Costa, J.E.R., Zodi Vaz, A.M., and Dennis, B.R., Solar burst with millimetre-wave emission at high frequency only, *Nature,* 1985, vol. 313, pp. 380–382. https://doi.org/10.1038/313380a0

Kaufmann, P., Costa, J.E.R., Gimenez De Castro, C.G., Hadano, Y.R., Kingsley, J.S., Kingsley, R.K., Levato, H., Marun, A., Raulin, J.-P., Rovira, M., Correia, V., and Silva, A.V.R., The new submillimeter-wave solar telescope, in *Proc. 2001 SBMO/IEEE MTT-S Int. Microwave and Optoelectron. Conf.,* 2001, pp. 439–442. https://doi.org/10.1109/SBMOMO.2001.1008800.

Kaufmann, P., Castro, C.G.G., Makhmutov, V.S., Raulin, J.-P., Schwenn, R., Levato, H., and Rovira, M., Launch of solar coronal mass ejections and submillimeter pulse bursts, *J. Geophys. Res.,* 2003, vol. 108, no. A7, p. 1280. https://doi.org/10.1029/2002JA009729

Kaufmann, P., Raullin, J.-P., de Castro, C.G.G., et al., A new solar burst spectral component emitting only in the terahertz range, *Astrophys. J.,* 2004, vol. 603, pp. L121–L124. https://doi.org/10.1086/383186

Kaufmann, P., Marcon, R., Abrantes, A., Bortolucci, E.C., Fernandes, L.O.T., Kropotov, G.I., Kudaka, A.S., Machado, N., Marun, A., Nikolaev, V., Silva, A., da Silva, C.S., and Timofeevsky, A., THz photometers for solar flare observations from space, *Exp. Astron.,* 2014, vol. 37, pp. 579–598. https://doi.org/10.1007/s10686-014-9389-y

Kaufmann, P., White, S.M., Marcon, R., Kudaka, A.S., Cabezas, D.P., Cassiano, M.M., Francile, C., Fernandes, L.O.T., Hidalgo Ramirez, R.F., Luoni, M., Marun, A., Pereyra, P., and de Souza, R.V., Bright 30 THz impulsive solar bursts, *J. Geophys. Res.: Space Phys.,* 2015, vol. 120, p. 4155. https://doi.org/10.1002/2015JA021313

Kinnison, J., Vaughan, R., Hill, P., Raouafi, N., Guo, Y., and Pinkine, N., Parker solar probe: A mission to touch the Sun, *IEEE Aerospace Conf.,* 2020, pp. 1–14. https://doi.org/10.1109/AERO47225.2020.9172703

Kropotov, G. and Kaufmann, P., Terahertz photometers for observing solar flares from space, *Fotonika,* 2013, vol. 5, no. 41, pp. 40–50.

Kropotov, G.I., Shakhmin, A.A., Kaplunov, I.A., and Rogalin, V.E., Application of spectral instruments in optical production and scientific research, *Fotonika,* 2023, vol. 5, no. 17, pp. 378–393. https://doi.org/10.22184/1993-7296.FRos.2023.17.5.378.392

Krucker, S., Castro, C.G.G., Hudson, H.S., Trottet, G., Bastian, T.S., Hales, A.S., Kašparová, J., Klein, K.-L., Kretzschmar, M., Lüthi, T., Mackinnon, A., Pohjolainen, S., and White, S.M., Solar flares at submillimeter wavelengths, *Astron. Astrophys. Rev.,* 2013, vol. 21, p. 58. https://doi.org/10.1007/s00159-013-0058-3

Kvashnin, A.A., Logachev, V.I., Filippov, M.V., Makhmutov, V.S., Maksumov, O.S., Stozhkov, Yu.I., Kalinin, E.V., Orlov, A.A., Ozolin, V.V., Izmailov, G.N., Krivolapova, O.Yu., and Gaifutdinova, A.G., Optical system of the device for measuring solar terahertz radiation, *Kosm. Tekh. Tekhnol.,* 2021, vol. 4, no. 35, pp. 22–30.

Lüthi, T., Magun, A., and Miller, M., First observation of a solar X-class flare in the submillimeter range with KOSMA, *Astron. Astrophys.,* 2004, vol. 415, pp. 1123–1132.
https://doi.org/10.1051/0004-6361:20034624

Makhmutov, V.S., Raulin, J.-P., Castro, C.G.G., Kaufmann, P., and Correia, E., Wavelet decomposition of submillimeter solar radio bursts, *Sol. Phys.,* 2003, vol. 218, pp. 211–220.
https://doi.org/10.1023/B:SOLA.0000013047.26419.33

Makhmutov, V.S., Kurt, V.G., Yushkov, B.Yu., Grechnev, V.V., Kaufmann, P., Raulin, J.-P., Bazilevskaya, G.A., and Stozhkov, Yu.I., Spectral peculiarities of high energy X-ray radiation, gamma radiation, and Submillimeter radio emission in the impulsive phase of a solar flare, *Bull. Russ. Acad. Sci. Phys.,* 2011, vol. 75, no. 6, pp. 747–750.

Philippov, M.V., Makhmutov, V.S., Maksumov, O.S., Kvashnin, A.A., Kalinin, E.V., Logachev, V.I., Gaifutdinova, A.G., Krivolapova, O.Yu., Sokov, S.V., and Mizin, S.V., Study of the temperature effect of resonant optical choppers in space scientific equipment, *Kosm. Tekh. Tekhnol.,* 2023a, vol. 1, no. 40, pp. 30–40. https://www.elibrary.ru/wzamjn.

Philippov, M.V., Makhmutov, V.S., Logachev, V.I., and Razumeyko, M.V., Preliminary calculation of sensitivity of detectors for the future space experiment "Sun-Terahertz," *Tech. Phys.,* 2023b, vol. 68, no. 9, pp. 1281–1286.
https://doi.org/10.61011/TP.2023.09.57369.167-23

Philippov, M.V., Logachev, V.I., Makhmutov, V.S., Razumeiko, M.V., Gaifutdinova, A.G., and Krivolapova, O.Yu., Calculation of solar terahertz radiation fluxes recorded by scientific receivers on board the International Space Station, *Kosm. Tekh. Tekhnol.,* 2024a, vol. 2, no. 45, pp. 68–83.
https://www.elibrary.ru/xdheun.

Philippov, M.V., Makhmutov, V.S., and Razumeiko, M.V., Scientific equipment for the space experiment "Sun-Terahertz": Study of the temperature effect of the Golay cell, *Izmerit. Tekh.,* 2024b, no. 3, pp. 20–25.
https://doi.org/10.32446/0368-1025it.2024-3-20-25

Philippov, M.V., Makhmutov, V.S., Maksumov, O.S., Kvashnin, A.A., Kvashnin, A.N., Razumeiko, M.V., Logachev, V.I., Mizin, S.V., and Sokov, S.V., Electronics unit for scientific equipment "Sun-Terahertz," *Pribory Tekh. Eksp.,* 2024c, no. 3, pp. 108–117.

Wedemeyer, S., Bastian, T., Brajša, R., Hudson, H., Fleishman, G., Loukitcheva, M., Fleck, B., Kontar, E.P., De Pontieu, B., Yagoubov, P., Tiwari, S.K., Soler, R., Black, J.H., Antolin, P., Scullion, E., Gunár, S., Labrosse, N., Ludwig, H.-G., Benz, A.O., White, S.M., Hauschildt, P., Doyle, J.G., Nakariakov, V.M., Ayres, T., Heinzel, P., Karlický, M., Van Doorsselaere, T., Gary, D., Alissandrakis, C.E., Nindos, A., Solanki, S.K., Rouppe van der Voort, L., Shimojo, M., Kato, Y., Zaqarashvili, T., Perez, E., Selhorst, C.L., and Bárta, M., Solar science with the Atacama Large Millimeter/Submillimeter Array—a new view of our Sun, *Space Sci. Rev.,* 2016, vol. 200, pp. 1–73.
https://doi.org/10.1007/s11214-015-0229-9

Yasuko, K. and Takamasa, S., Atmospheric propagation model of terahertz-wave, *J. Natl. Inst. Inf. Commun. Technol.,* 2008, vol. 55, no. 1, pp. 73–77.

Publisher's Note. Pleiades Publishing remains neutral with regard to jurisdictional claims in published maps and institutional affiliations.
AI tools may have been used in the translation or editing of this article.